European Journal of Computational Mechanics, 2014
Vol. 23, Nos. 3–4, 113–137, http://dx.doi.org/10.1080/17797179.2014.882140

Taylor & Francis
Taylor & Francis Group

Stokes–Darcy coupling in severe regimes using multiscale stabilisation for mixed finite elements: monolithic approach versus decoupled approach

L. Abouorm*, R. Troian, S. Drapier, J. Bruchon and N. Moulin

Mechanics and Materials Science Division & LGF CNRS UMR 5307, École Nationale Superieure des Mines de Saint-Étienne, Saint-Étienne, France

The article exposes robust finite element solutions for coupling flows in both purely fluid region, ruled by Stokes equations, and a porous region of low permeability (down to $10^{-15}\,m^2$) governed by Darcy's equations. Relying on stabilised FE formulations, two different numerical strategies are investigated for coupling Stokes–Darcy flows: a decoupled strategy, based on the use of two matching meshes and two finite element spaces for discretising the Stokes–Darcy coupled system; a unified or monolithic strategy, consisting in defining one single mesh for discretising the computational domain, associated with one single finite element space. In the first case, P1+/P1 mixed finite element is used for both Stokes and Darcy (primal form), while P1/P1 approximation is used in the second case with the dual form of the Stokes–Darcy coupled problem stabilised by a variational multi-scale method. The method of manufactured solution is used to evaluate the convergence rates of the solutions and the code robustness. Then, cases of flows normal and tangential to the Stokes–Darcy interface are investigated, and a comparison with available analytical solutions is carried out. Capabilities of both approaches are then demonstrated in solving problems with complex geometry and 3D cases.

Keywords: infusion; Stokes–Darcy coupled problem; monolithic approach; decoupled approach; ASGS; P1+/P1

1. Introduction

This paper proposes a comparison of two methods capable of dealing with the Stokes–Darcy coupled problem. The Stokes–Darcy coupled problem has been studied by many researchers in many field of engineering. The numerical applications proposed in this paper are in the field of resin infusion processes. The specificity of such applications is the low permeability of the Darcy zone and the thin thickness of the Stokes layer. The strategies studied in this contribution for solving the coupled Stokes–Darcy problem are the decoupled (Celle, Drapier, & Bergheau, 2008a, 2008b) and monolithic (Pacquaut, Bruchon, Moulin, & Drapier, 2012) approaches. The decoupled strategy consists in using two different meshes matching at the interface to solve the Stokes and the Darcy equations and to equilibrate velocity and pressure iteratively (Discacciati & Quarteroni, 2009). For this, special methods for prescribing interface conditions between the two media have to be introduced. Conversely, the originality of the monolithic approach consists in using a single non-necessarily structured mesh and the same finite element spaces in Stokes and Darcy domains. A level-set function is used

*Corresponding author. Email: lara_bouorm@hotmail.com

to represent the interface between Stokes and Darcy and, interface conditions are included into the weak formulation, and naturally satisfied. For both methods, mixed finite elements in velocity and pressure are used in the whole domain. A $P1/P1$ (piecewise linear in both velocity and pressure for a simplicial mesh) continuous approximation is employed throughout the entire domain. To ensure the unicity of the solution, the finite element pairs for pressure and velocity should verify Brezzi–Babuska conditions or some additional terms (depending on the size of mesh and finite element residual) should be added to the discrete variational formulation of the problem to satisfy Babuska theorem. In literature, different pairs of elements are used to couple Stokes–Darcy problem for decoupled and monolithic approaches. The difficulty of the choice of stable elements for Stokes–Darcy coupled problem is that the stable elements for Stokes are not stable for Darcy and vice versa. Because of the condition on the finite element spaces, coupling of different finite elements can be compatible for the decoupled strategy and uncompatible for unified strategies.Briefly, it does not exist a standard stable finite element pair for both Stokes and Darcy. The choice of different stable pairs (defined in two different discretised spaces) succeeds in decoupled approach where every domain is represented by a mesh independently from the other domain. For the decoupled approach, Discacciati and Quarteroni (2009) couples Taylor-Hood elements for Stokes with C^0 Lagrangian for Darcy, and Layton, schieweck, and Yotov (2003) couples Taylor-Hood elements for Stokes with Raviart–Thomas (RT) elements for Darcy. In this paper, the decoupled approach uses a $P1/P1$ formulation stabilised with hierarchical bubble functions, i.e. $P1+/P1$ finite element for both equations of Stokes and primal Darcys formulation.

For the monolithic approach, Burman and Hansbo (2007) couples P1/P0 elements with pressure stabilisation in Stokes and Darcy domains, Layton et al. (2003) couples Taylor-Hood elements or MINI-elements for Stokes with Brezzi–Douglas–Marini or RT elements in Darcy and Pacquaut et al. (2012) couples MINI-elements for Stokes with Hughes variational multiscale stabilised elements for Darcy. The last method proposed in Pacquaut et al.'s (2012) works in standard cases (flow parallel to the interface, high permeabilities $K > 10^{-8}\,\mathrm{m}^2$) but shows oscillations, accuracy problems and bad behaviour in severe cases (complex geometries with curved interfaces in two-dimensional (2D) and three-dimensional (3D) cases, low permeabilities $10^{-8}\mathrm{m}^2 \leq K \leq 10^{-15}\,\mathrm{m}^2$). The aim of this paper is to present a monolithic approach based on P1/P1 formulation for Stokes and the dual formulation of Darcy stabilised with algebraic subgrid scale (ASGS) method (Badia & Codina, 2008, 2010) which remains effective in severe cases, and assess along with a decoupled approach that has been proved to be robust in standard cases (Celle et al., 2008b).

This paper is organised as follows. Section 2 presents the mathematical modelling for the Stokes–Darcy coupled problem, the physical assumptions and the coupling physical conditions between the Stokes and Darcy equations. Sections 3 and 4 introduce, respectively, the monolithic approach stabilised with a variational multiscale (VMS) method and the decoupled approach based on P1+/P1 formulation in Stokes and Darcy. In Section 5, we study the rate of convergence of monolithic and decoupled approaches by using manufactured solutions and we compare the orders of convergence obtained with each method. Section 6 presents a comparison between monolithic and decoupled approaches for a flow perpendicular to the interface, a flow parallel to the interface and a flow with inclined interface. Finally, Section 7 presents numerical simulations in 2D and 3D for complex geometries such as those met in liquid moulding in manufacturing processes of composite materials.

2. Mathematical model

2.1. Mathematical formulation of the physical problem

Let Ω be a bounded domain of $\mathbb{R}^m$, divided into two non-overlapping subdomains, Ω_s and Ω_d, separated by a surface $\Gamma = \bar{\Omega}_s \cap \bar{\Omega}_d$ (see Figure 1). The problem is to describe the flow of an incompressible Newtonian fluid ruled by the Stokes equations in Ω_s and by the Darcy equations in Ω_d which is assumed to be a porous medium. In the following, index s is used to denote everything that concerns the Stokes domain and index d for the Darcy domain.

In Ω_s, Stokes equations (momentum and mass conservation), completed with Dirichlet and Neumann boundary conditions are

$$\begin{aligned} -\nabla \cdot (2\eta \dot{\varepsilon}(\mathbf{v_s})) + \nabla p_s &= \mathbf{f_s} \quad \text{in} \quad \Omega_s \\ -\nabla \cdot \mathbf{v_s} &= h_s \quad \text{in} \quad \Omega_s \\ \mathbf{v_s} &= \mathbf{v}^1 \quad \text{on} \quad \Gamma_{s,D} \\ \sigma \cdot \mathbf{n_s} &= \mathbf{t} \quad \text{on} \quad \Gamma_{s,N} \end{aligned} \tag{1}$$

where $\mathbf{v_s}$ is the velocity field, $\dot{\varepsilon}(\mathbf{v_s})$ is the strain rate tensor defined by $\dot{\varepsilon}(\mathbf{v_s}) = \frac{1}{2}(\nabla \mathbf{v_s} + \nabla^T \mathbf{v_s})$, $\mathbf{f_s}$ denotes the volume forces, $\mathbf{n_s}$ is the unit vector normal to the boundary of Ω_s, $\mathbf{t}$ is the stress vector to be prescribed on $\Gamma_{s,N}$ and η is the fluid viscosity, assumed to be constant (Newtonian fluid assumption). If the fluid is incompressible then $h_s = 0$.

The Darcy equations in Ω_d are given in a mixed form by

$$\begin{aligned} \tfrac{\eta}{K}\mathbf{v_d} + \nabla p_d &= \mathbf{f_d} \quad \text{in} \quad \Omega_d \\ -\nabla \cdot \mathbf{v_d} &= h_d \quad \text{in} \quad \Omega_d \\ \mathbf{v_d} \cdot \mathbf{n_d} &= v^2 \quad \text{on} \quad \Gamma_{d,D} \\ p_d &= p_{ext} \quad \text{on} \quad \Gamma_{d,N} \end{aligned} \tag{2}$$

In this paper, the medium is assumed to be isotropic, consequently the permeability K is a scalar. p_{ext} is a pressure to be prescribed on $\Gamma_{d,N}$, $\mathbf{n_d}$ is the outward unit vector normal to the boundary of Ω_d and $\mathbf{f_d}$ is the volume force vector.

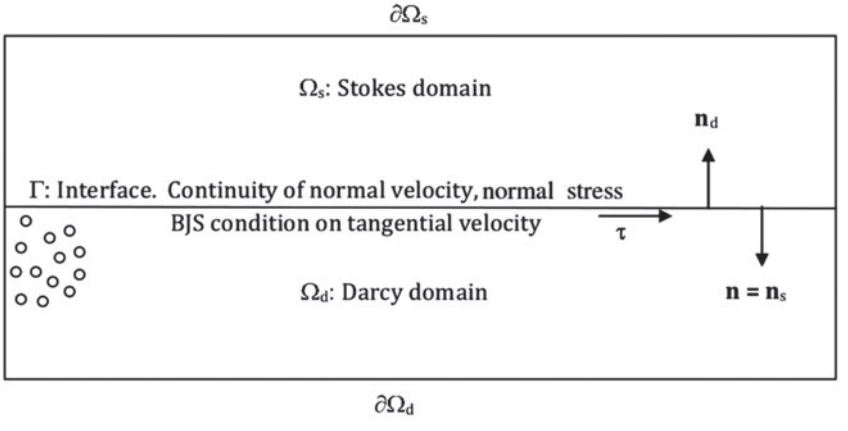

Figure 1. Computational domain for Stokes–Darcy coupling, 2D representation.

2.2. Coupling conditions

Moreover, coupling conditions must be considered on the interface Γ of normal $\mathbf{n} = \mathbf{n_s}$.

Continuity of normal velocity

The mass conservation across interface Γ is expressed by the continuity of the normal velocity field $\mathbf{v}$:

$$\mathbf{v_s} \cdot \mathbf{n_s} + \mathbf{v_d} \cdot \mathbf{n_d} = 0 \quad \text{on} \quad \Gamma \tag{3}$$

Continuity of the fluid normal stress

$$\mathbf{n} \cdot \sigma_\mathbf{s} \cdot \mathbf{n} = \mathbf{n} \cdot \sigma_\mathbf{d} \cdot \mathbf{n} \quad \text{on} \quad \Gamma \tag{4}$$

Beaver–Joseph–Saffman condition (Beavers & Joseph, 1967)

The Beaver–Joseph–Saffman condition allows the tangential velocity to be specified on the interface Γ, it writes

$$2\mathbf{n} \cdot \dot{\varepsilon}(\mathbf{v_s}) \cdot \boldsymbol{\tau}_\mathbf{j} = -\frac{\alpha}{\sqrt{K}}(\mathbf{v_s} \cdot \boldsymbol{\tau}_\mathbf{j}), \quad j = 1, 2 \tag{5}$$

where α is a dimensionless parameter, so-called slip coefficient and $\boldsymbol{\tau}_\mathbf{j}$ are the vectors tangent to the interface.

3. Monolithic approach

This section focuses on coupling Stokes–Darcy by using one single mesh for both fluid and porous domains. The discretisation is ensured by using a mixed velocity–pressure finite element formulation. Velocity and pressure are approximated by piecewise linear and continuous functions and the formulation is stabilised with the ASGS method developed in Badia and Codina (2008, 2010).

In the Eulerian monolithic framework considered here, the interface Γ separating the purely fluid domain and the porous domain is not described by a set of element boundaries. Conversely, using a level set function (Bruchon, Digonnet, & Coupez, 2009; Osher, 1988; Sussman, Smereka, & Osher, 1994), this interface passes throughout the mesh elements. The location of each physical domain as well as the location of their interfaceis known through an additional function, ϕ, defined as a signed distance function to the interface:

$$\phi(x) = \begin{cases} \min\limits_{x_1 \in \Gamma} \|x - x_1\| & \text{if} \quad x \in \Omega_s \\ -\min\limits_{x_1 \in \Gamma} \|x - x_1\| & \text{if} \quad x \notin \Omega_s \end{cases} \tag{6}$$

This definition corresponds to a level-set setting, and the Stokes–Darcy interface is consequently described as the zero-level isosurface of $\phi : \Gamma = \{\phi = 0\}$. In this paper, only steady states are considered; however, this definition allows for an 'easy' numerical treatment of the interface motion when considering the deformation of the porous medium. When considering the discrete problem, ϕ is approximated by ϕ_h which is continuous and piecewise linear on Ω_h. As established in papers dedicated to this method (Bruchon et al., 2009; Osher, 1988; Sussman et al., 1994), Equation (6) allows us to compute some important geometrical properties on the interface Γ, such as the normal $\mathbf{n}$ which is calculated as: $\mathbf{n} = \frac{\mathbf{V}\phi}{\|\mathbf{V}\phi\|}$.

3.1. Weak formulation

In order to solve the Stokes–Darcy coupled problem by a finite element method, the weak formulation has to be established. We present the weak formulation of Stokes and Darcy separately. The weak formulation of the coupled problem is then obtained by summing up the weak formulation of Stokes and Darcy taking into consideration interface conditions described in Section 2.2. For the sake of simplicity, we choose to write the L^2 inner product in $\Omega_{s,d}$ as $\langle \cdot, \cdot \rangle$.

The spaces of velocity, pressure and test functions defined here correspond to the functional setting of Stokes–Darcy coupled problem, with the dual formulation of Darcy's problem. These spaces are taken as

$$\begin{aligned} Q_i = L^2(\Omega_i) &= \left\{ p, \int_{\Omega_i} p^2 d\Omega < \infty \right\} \\ V_s &= \{ \mathbf{v} \in H^1(\Omega_s)^m \mid \mathbf{v} = \mathbf{v^1} \text{ on } \Gamma_{s,D} \} \\ V_{0,s} &= \{ \mathbf{v} \in H^1(\Omega_s)^m \mid \mathbf{v} = 0 \text{ on } \Gamma_{s,D} \} \\ H^1(\Omega_s)^m &= \{ \mathbf{v} \in L^2(\Omega_s)^m, \nabla \mathbf{v} \in L^2(\Omega_s)^{m \times m} \}, \\ V_d &= \{ \mathbf{v} \in H(div, \Omega_d) \mid \mathbf{v} \cdot \mathbf{n} = v^2 \text{ on } \Gamma_{d,D} \} \\ V_{0,d} &= \{ \mathbf{v} \in H(div, \Omega_d) \mid \mathbf{v} \cdot \mathbf{n} = 0 \text{ on } \Gamma_{d,D} \} \\ H(div, \Omega_d) &= \{ \mathbf{v} \in L^2(\Omega_d)^m \mid \nabla \cdot \ \mathbf{v} \in L^2(\Omega_d) \} \end{aligned} \tag{7}$$

with $i = s$ or $i = d$ and m is the dimension equal to 2 or 3.

The variational formulation of the Stokes problem consists in finding a velocity–pressure pair $[\mathbf{v_s}, p_s] \in V_s \times Q_s$ such that:

$$B_s([\mathbf{v_s}, p_s], [\mathbf{w_s}, q_s]) = L_s([\mathbf{w_s}, q_s]) \tag{8}$$

for any $\mathbf{w_s}$ and q_s weighting functions defined in $V_{0,s}$ and Q_s respectively. The bilinear form B_s and the linear form L_s are defined in Stokes by:

$$\begin{aligned} B_s([\mathbf{v_s}, p_s], [\mathbf{w_s}, q_s]) = 2\eta \langle \dot{\boldsymbol{\varepsilon}}(\mathbf{v_s}), \dot{\boldsymbol{\varepsilon}}(\mathbf{w_s}) \rangle - \langle p_s, \nabla \cdot \mathbf{w_s} \rangle + \langle \nabla \cdot \mathbf{v_s}, q_s \rangle \\ + \langle p_d, \mathbf{w_s} \cdot \mathbf{n_s} \rangle_\Gamma + \langle \frac{\alpha \eta}{\sqrt{K}} (\mathbf{v_s} \cdot \boldsymbol{\tau}), (\mathbf{w_s} \cdot \boldsymbol{\tau}) \rangle_\Gamma \end{aligned} \tag{9}$$

$$L_s([\mathbf{w_s}, q_s]) = \langle \mathbf{f_s}, \mathbf{w_s} \rangle + \langle h_s, q_s \rangle + \langle p_{ext,s} \mathbf{n_s}, \mathbf{w_s} \rangle_{\Gamma_{s,N}} \tag{10}$$

The variational formulation of the Darcy problem consists in finding a velocity–pressure pair $V_d \times Q_d$ such that:

$$B_d([\mathbf{v_d}, p_d], [\mathbf{w_d}, q_d]) = L_d([\mathbf{w_d}, q_d]) \tag{11}$$

for any $\mathbf{w_d}$ and q_d weighting functions defined in $V_{0,d}$ and Q_d. The bilinear form B_d and the linear form L_d are defined in Darcy by:

$$B_d([\mathbf{v_d}, p_d], [\mathbf{w_d}, q_d]) = \frac{\eta}{K} \langle \mathbf{v_d}, \mathbf{w_d} \rangle - \langle p_d, \nabla \mathbf{w_d} \rangle + \langle q_d, \nabla \mathbf{v_d} \rangle + \langle p_d, \mathbf{w_d} \cdot \mathbf{n_d} \rangle_{\Gamma_{d,N}} \tag{12}$$

$$L_d([\mathbf{w_d}, q_d]) = \langle \mathbf{f_d}, \mathbf{w_d} \rangle + \langle h_d, q_d \rangle + \langle p_{ext,d} \mathbf{n}, \mathbf{w_d} \rangle_{\Gamma_{d,N}} \tag{13}$$

The mixed formulation of the Stokes–Darcy problem is established by considering a velocity $\mathbf{v}$ on Ω and a pressure field p on Ω such as $\mathbf{v}_{|\Omega_i} = \mathbf{v}_i$ and $p_{|\Omega_i} = p_i$ with $i = s$ or $i = d$. The mixed weak formulation of Stokes–Darcy is obtained by summing up

Equations (9) and (12) and taking into consideration the conditions enforced on the Stokes–Darcy interface described in Section 2.2. Hence, the variational formulation of the Stokes–Darcy coupled problem consists in finding $[\mathbf{v},p] \in V_c \times Q_c$ such that

$$B_c([\mathbf{v},p],[\mathbf{w},q]) = L_c([\mathbf{w},q])$$

where $[\mathbf{w},q]$ are weighting functions defined in $V_{0,c} \times Q_c$.

$$V_c = V_s \times V_d$$

$$V_{0,c} = V_{0,s} \times V_{0,d}$$

$$Q_c = Q_s \times Q_d$$

The bilinear form B_c and the linear form L_c are defined by

$$B_c([\mathbf{v},q],[\mathbf{w},q]) = \langle 2\eta\dot{\boldsymbol{\varepsilon}}(\mathbf{v}) : \dot{\boldsymbol{\varepsilon}}(\mathbf{w})H_s\rangle_\Omega + \langle \frac{\eta}{K}\ \mathbf{v},\mathbf{w}\ H_d\rangle_\Omega - \langle p, \boldsymbol{\nabla}\cdot\mathbf{w}\rangle_\Omega + \langle q,\ \boldsymbol{\nabla}\cdot\mathbf{v}\rangle_\Omega + \langle \frac{\alpha\eta}{\sqrt{K}}\ \mathbf{v},\mathbf{w}\rangle_\Gamma \tag{14}$$

$$L_c([\mathbf{v},p],[\mathbf{w},q]) = \langle \mathbf{f_c},\mathbf{w}\rangle_\Omega + \langle h_c,q\rangle_\Omega + \langle \mathbf{t_s},\mathbf{w}\rangle_{\Gamma_{s,N}} + \langle p_{ext},\mathbf{w}\rangle_{\Gamma_{d,N}} \tag{15}$$

$(\mathbf{f_c}, h_c)$ are defined by $(\mathbf{f_d}, h_d)$ in Darcy and $(\mathbf{f_s}, h_s)$ in Stokes and $h_c = (h_s,\ h_d)$. H_i is a Heaviside function equal to 1 in domain i and vanishing elsewhere.

3.2. *Finite element approximation with ASGS stabilisation*

The whole computational domain $\Omega \subset \mathrm{R}^m$ is discretised with one single unstructured mesh. This mesh is made up of n_e triangles if $m = 2$ and of n_e tetrahedrons if $m = 3$. Let V_h and Q_h be the finite element spaces of the piecewise linear and continuous functions, which contain the solutions $\mathbf{v_{h,i}}$ and $p_{h,i}$. The Galerkin approximation of both Stokes and Darcy problems requires the use of velocity–pressure interpolation that satisfy the adequate *inf-sup* condition. Different interpolation pairs are known to satisfy this condition for each problem independently, but the key issue is to find interpolations that satisfy both at the same time. In the case of the Stokes–Darcy problem, the issue is impossible to address with standard finite elements within the framework of Brezzi–Babuska theory. That is why, in this paper, stabilised finite element methods are used. The philosophy of the stabilised methods is to strengthen classical variational formulations so that discrete approximations which would otherwise be unstable become stable and convergent. Over the last decades, a formal framework has been developed for stabilising finite element formulations, based on VMS techniques. This framework is introduced by Hughes (1995) or Hughes, Feijóo, Mazzei, and Quincy (1998). On this basis, a VMS method has been developed by Badia and Codina to stabilise the Stokes–Darcy coupled problem (Badia & Codina, 2008, 2010). The monolithic approach presented in this paper is based on this VMS technique. The basic idea of this method is to approximate the local effects of the component of the continuous solution which cannot be captured by the finite element solution. It consists in splitting the continuous solution for velocity and pressure into two components, one coarse corresponding to the finite element scale $[\mathbf{v_h}, p_h]$, and a finer component corresponding to lower scale fields $[\mathbf{v}', p']$. The velocity is decomposed as $\mathbf{v} = \mathbf{v_h} + \mathbf{v}'$ and the pressure field is decomposed as $p = p_h + p'$. We consider therefore a subgrid

space $V' \times Q'$ such that $V \times Q = (V_h \times Q_h) \oplus (V' \times Q')$. Invoking this decomposition in the continuous problem (Equation (14)) for both solution and test functions, one gets the two-scales systems

$$B_c([\mathbf{v_h}, p_h]), [\mathbf{w_h}, q_h]) + B_c([\mathbf{w}', p'], [\mathbf{w_h}, q_h]) = L_c([\mathbf{w_h}, q_h]) \tag{16}$$

$$B_c([\mathbf{v_h}, p_h], [\mathbf{w}', p']) + B_c([\mathbf{v}', p'], [\mathbf{w}', q']) = L_c([\mathbf{w}', q']) \tag{17}$$

for all $[\mathbf{w_h}, q_h] \in V_h \times Q_h$ and $[\mathbf{w}', q'] \in V' \times Q'$. After approximating Equation (17) with an algebraic formulation, by introducing the operator of projection P' onto $V' \times Q'$, the approximated fields $[\mathbf{v}', p']$ are taken into account in the finite element problem (Equation (16)). We get the stabilised forms of the bilinear and linear forms in Stokes, Darcy and Stokes–Darcy coupled problem.

The stabilised problem in Stokes can be written as follows.

Find $[\mathbf{v_{s,h}}, p_{s,h}] \in V_h \times Q_h$ such as

$$B_{s,stable}([\mathbf{v_{s,h}}, p_{s,h}], [\mathbf{w_{s,h}}, q_{s,h}]) = L_{s,stable}([\mathbf{w_{s,h}}, q_{s,h}]) \tag{18}$$

where the bilinear stabilised form $B_{s,stable}$ and the linear stabilised form $L_{s,stable}$ are defined by

$$\begin{aligned} &B_{s,stable}([\mathbf{v_{s,h}}, p_{s,h}], [\mathbf{w_{s,h}}, q_{s,h}]) \\ &\quad = B_s([\mathbf{v_{s,h}}, p_{s,h}], [\mathbf{w_{s,h}}, q_{s,h}]) + \sum_{e=1}^{n_e} \tau_q \langle P'_{h,p}(\nabla \cdot \mathbf{v_{s,h}}), \nabla \cdot \mathbf{w_{s,h}} \rangle_{\Omega_h^e} \\ &\qquad + \sum_{e=1}^{n_e} \tau_v \langle P'_{h,u}(-\eta \Delta \mathbf{v_{s,h}} + \nabla(div \mathbf{v_{h,s}})) + \nabla p_{s,h}), \eta \Delta \mathbf{w_{s,h}} \rangle_{\Omega_h^e} \\ &\qquad + \sum_{e=1}^{n_e} \tau_v \langle P'_{h,u}(-\eta \Delta \mathbf{v_{s,h}} + \nabla(div(\mathbf{v_{h,s}})) + \nabla p_{s,h}), +\nabla q_{s,h} \rangle_{\Omega_h^e} \end{aligned} \tag{19}$$

$$\begin{aligned} L_{s,stable}([\mathbf{w_{s,h}}, q_{s,h}]) = L_s([\mathbf{w_{s,h}}, q_{s,h}]) &+ \sum_{e=1}^{n_e} \tau_q \langle P'_{h,p}(h_s), \nabla \cdot \mathbf{w_{s,h}} \rangle_{\Omega_h^e} \\ &+ \sum_{e=1}^{n_e} \tau_v \langle P'_{h,p}(\mathbf{f_s}), -\nabla(div(\mathbf{v_{h,s}})) + \eta \Delta \mathbf{w_{s,h}} - \nabla q_{s,h} \rangle_{\Omega_h^e} \end{aligned} \tag{20}$$

with $\sum_{n_e}$ which denotes the sum over the n_e mesh elements and $\langle \cdot, \cdot \rangle_{\Omega_h^e}$ is the $L^2(\Omega_h^e)$ inner product on every element Ω_h^e. $B_s([\mathbf{v_{s,h}}, p_{s,h}], [\mathbf{w_{s,h}}, q_{s,h}])$ and $L_s([\mathbf{w_{s,h}}, q_{s,h}])$ are defined in Equation (9). τ_q, τ_v are the stabilisation parameters (obtained by Fourier transform) that we compute at the element scale as (Equation (21)) (Badia & Codina, 2008):

$$\begin{aligned} \tau_q &= c_1 \, \eta \\ \tau_v &= \frac{1}{c_1 \eta} \, h_k^2 \end{aligned} \tag{21}$$

where c_1 is an algorithmic constant and h_k is the characteristic size of the element. $P'_{h,u}$ is the broken L^2 projection onto V' and $P'_{h,p}$ is the broken L^2 projection onto Q'. The simplest approach is to take P'_h as the identity operator when acting on the FE residual. Assuming this, one obtains the stabilised method referred to as ASGS method. In addition, the velocity is linear and continuous (P1 element), then

$\Delta(\mathbf{w_{h,s}}) - \nabla(div(\mathbf{w_{h,s}})) = 0$. Invoking this, one gets the following stabilised forms B_s and L_s in Stokes:

$$B_{s,stable}([\mathbf{v_{s,h}}, p_{s,h}], [\mathbf{w_{s,h}}, q_{s,h}]) = B_s([\mathbf{v_{s,h}}, p_{s,h}], [\mathbf{w_{s,h}}, q_{s,h}]) + \sum_{e=1}^{n_e} \tau_q \langle \nabla \cdot \mathbf{v_{s,h}}, \nabla \cdot \mathbf{w_{s,h}} \rangle_{\Omega_h^e} + \sum_{e=1}^{n_e} \tau_v \langle \nabla p_{s,h}, +\nabla q_{s,h} \rangle_{\Omega_h^e} \tag{22}$$

$$L_{s,stable}([\mathbf{w_{s,h}}, q_{s,h}]) = L_s([\mathbf{w_{s,h}}, q_{s,h}]) + \sum_{e=1}^{n_e} \tau_q \langle h, \nabla \cdot \mathbf{w_{s,h}} \rangle_{\Omega_h^e} + \sum_{e=1}^{n_e} \tau_v \langle \mathbf{f_s}, +\nabla q_{s,h} \rangle_{\Omega_h^e} \tag{23}$$

Similary by using the ASGS method, the stabilised problem in Darcy can be written as follows: Find $[\mathbf{v_{d,h}}, p_{d,h}] \in V_h \times Q_h$ such as

$$B_{d,stable}([\mathbf{v_{d,h}}, p_{d,h}][\mathbf{w_{d,h}}, q_{d,h}]) = L_{d,stable}([\mathbf{w_{d,h}}, q_{d,h}]) \tag{24}$$

$$B_{d,stable}([\mathbf{v_{d,h}}, p_{d,h}], [\mathbf{w_{d,h}}, q_{d,h}]) = B_d([\mathbf{v_{d,h}}, p_{d,h}], [\mathbf{w_{d,h}}, q_{d,h}] + \sum_{e=1}^{n_e} \tau_p \langle \nabla \cdot \mathbf{v_{d,h}}, \nabla \cdot \mathbf{w_{d,h}} \rangle_{\Omega_h^e} + \sum_{e=1}^{n_e} \tau_u \langle \frac{\eta}{K} \mathbf{v_{d,h}} + \nabla p_{d,h}, -\frac{\eta}{K} \mathbf{w_{d,h}} + \nabla q_{d,h} \rangle_{\Omega_h^e} \tag{25}$$

$$L_{d,stable}([\mathbf{w_{d,h}}, q_{d,h}]) = L_d([\mathbf{w_{d,h}}, q_{d,h}]) + \sum_{e=1}^{n_e} \tau_p \langle h_d, \nabla \cdot \mathbf{w_{d,h}} \rangle_{\Omega_h^e} + \sum_{e=1}^{n_e} \tau_u \langle \mathbf{f_d}, -\frac{\eta}{K} \mathbf{w_{h,d}} + \nabla q_{d,h} \rangle_{\Omega_h^e} \tag{26}$$

where $B_d([\mathbf{v_{d,h}}, p_{d,h}], [\mathbf{w_{d,h}}, q_{d,h}])$ and $L_d([\mathbf{w_{d,h}}, q_{d,h}])$ are defined in (12). τ_p, τ_u are the stabilisation parameters that we compute at the element level as (Equation (27)) (Badia & Codina, 2008)

$$\tau_p = c_p \frac{\eta}{k} l_p^2$$

$$\tau_u = \left(c_u \frac{\eta}{K} l_u^2 \right)^{-1} h_k^2 \tag{27}$$

with c_p and c_u as some algorithmic constants. l_u and l_p are length scales which we choose to take $(L_0 h_k)^{1/2}$, L_0 is the characteristic length of the domain and h_k is the element size.

For Stokes and Darcy flows coupled through their interfaces, the stabilised problem with ASGS can be written as follows.

Find $[\mathbf{v_h}, p_h] \in V_h \times Q_h$ such that:

$$B_{c,stable}([\mathbf{v_h}, p_h][\mathbf{w_h}, q_h]) = L_{c,stable}([\mathbf{w_h}, q_h]) \quad \forall [\mathbf{w_h}, q_h] \in V_h \times Q_h \tag{28}$$

$$B_{c,stable}([\mathbf{v_h}, p_h], [\mathbf{w_h}, q_h]) = B_c([\mathbf{v_h}, p_h], [\mathbf{w_h}, q_h]) + \sum_{e=1}^{n_e} \tau_{p,c} \langle \nabla \cdot \mathbf{v_h}, \nabla \cdot \mathbf{w_h} \rangle_{\Omega_h^e} + \sum_{e=1}^{n_e} \tau_{u,c} \langle H_d \frac{\eta}{K} \mathbf{v_h} + \nabla p_h, -H_d \frac{\eta}{K} \mathbf{w_h} + \nabla q_h \rangle_{\Omega_h^e} \tag{29}$$

$$L_{c,stable}([\mathbf{w_h}, q_h]) = L_c([\mathbf{w_h}, q_h]) + \sum_{e=1}^{n_e} \tau_{p,c} \langle h_c, \nabla \cdot \mathbf{w_h} \rangle_{\Omega_h^e} + \sum_{e=1}^{n_e} \tau_{u,c} < \mathbf{f_c}, -H_d \frac{\eta}{K} \mathbf{w_h} + \nabla q_h >_{\Omega_h^e} \tag{30}$$

$\tau_{p,c}$, $\tau_{u,c}$ are the stabilisation parameters that we compute as (Equation (31)) (Badia & Codina, 2008)

$$\tau_{p,c} = c_p \frac{\eta}{K} l_p^2 H_d + c_1 \eta H_s$$

$$\tau_{u,c} = (c_1 \eta H_s + c_u \frac{\eta}{K} l_u^2 H_d)^{-1} h_k^2 \tag{31}$$

We have two ways for computing the surface integral $\int_\Gamma \alpha \frac{\eta}{\sqrt{K}} (\mathbf{v_h} \cdot \tau)(\mathbf{w_h} \cdot \tau)$: the transformation of this integral into volume integral by using a delta Dirac function or the direct computation of this integral on the interface Γ obtained by a linear approximation using the values of the level-set function ϕ. The exact computation of the surface integral shows more accurate results than Dirac approximation (Figure 7). Moreover, the Stokes and Darcy contributions are averaged over the elements cut by the interface Γ thanks to H_s and H_d. This approach could be improved by splitting these interface elements into Stokes and Darcy sub-elements (Pino Muñoz et al., 2013).

4. Decoupled approach

4.1. Weak formulation

The mixed weak formulation of the equations of Stokes and Darcy can take two different forms in which the boundary conditions on the pressure are prescribed as Dirichlet conditions or weakly, but more importantly can be stable or not with the chosen finite element discretisation (MINI-element, introduced in Arnold, Brezzi, and Fortin (1984)). Consequently, following the results from Celle et al. (2008a, 2008b), the dual mixed formulation is chosen for Stokes and the primal-mixed formulation is chosen for Darcy as proposed in Celle et al. (2008b) and (2008a). This choice ensures the stability of the systems discretised by using the MINI-element. The variational formulation of the Stokes problem consists in finding a velocity–pressure pair $[\mathbf{v_s}, p_s] \in V_s \times Q_s$ such that:

$$B_s^1([\mathbf{v_s}, p_s], [\mathbf{w_s}, q_s]) = L_s^1([\mathbf{w_s}, q_s]) \tag{32}$$

where $\mathbf{w_s}$ and q_s are the weighting functions defined in $V_{0,s}$ and Q_s, respectively. The bilinear form B_s^1 and the linear form L_s^1 are defined in Stokes by:

$$\begin{array}{rcl} B_s^1([\mathbf{v_s}, p_s][\mathbf{w_s}, q_s]) & = & 2\eta\ \langle \dot{\boldsymbol{\varepsilon}}(\mathbf{v_s}) : \dot{\boldsymbol{\varepsilon}}(\mathbf{w_s})\rangle_{\Omega_s} - \langle \nabla \cdot \mathbf{w_s}, p_s\rangle_{\Omega_s} - \langle \nabla \cdot \mathbf{v_s}, q_s\rangle_{\Omega_s} \\ L_s^1([\mathbf{w_s}, q_s]) & = & \langle \mathbf{f_s}, \mathbf{w_s}\rangle_{\Omega_s} + \langle h_s, q_s\rangle_{\Omega_s} + \langle \mathbf{t_s}, \mathbf{w_s}\rangle_{\Gamma_{s,N}} \end{array} \tag{33}$$

The variational formulation of the Darcy's problem consists in finding a velocity–pressure pair $[\mathbf{v_d}, p_d] \in L^2(\Omega_d)^m \times H^1(\Omega_d)$ such that:

$$B_d^1([\mathbf{v_d}, p_d], [\mathbf{w_d}, q_d]) = L_d^1([\mathbf{w_d}, q_d]) \tag{34}$$

where $\mathbf{w_d}$ and q_d are the weighting functions defined in $L^2(\Omega_d)^m$ and $H^{1,t}_{\Gamma}(\Omega_d)$. The bilinear form B_d and the linear form L_d are defined in Darcy by:

$$\begin{array}{c} B_d^1([\mathbf{v_d}, p_d][\mathbf{w_d}, q_d]) = \frac{\eta}{K}\langle \mathbf{v_d}, \mathbf{w_d}\rangle_{\Omega_d} + \langle \nabla p_d, \mathbf{w_d}\rangle_{\Omega_d} - \langle \nabla q_d, \mathbf{v_d}\rangle_{\Omega_d} \\ L_d^1([\mathbf{w_d}, q_d]) = \langle \mathbf{f_d}, \mathbf{w_d}\rangle_{\Omega_d} + \langle h_d, q_d\rangle_{\Omega_d} + \langle \mathbf{v_d} \cdot \mathbf{n_d}, q_d\rangle_{\Gamma_{d,N}} \end{array} \tag{35}$$

4.2. *Finite element approximation. Velocity and pressure discretisation*

For solving the flow problems, the computational domains $\Omega_s \subset R^m$ and $\Omega_d \subset R^m$ are discretised with meshes matching at the interface. These meshes are made up of triangles if $m = 2$ and of tetrahedra if $m = 3$. Let V_h and Q_h be the finite element spaces of the continuous piecewise linear functions, which contain the solutions $\mathbf{v_{h,i}}$ and $p_{h,i}$.

Like for the monolithic formulation, flows have to be stabilised, and here another type of sub-grid scale stabilisation is employed (Arnold et al., 1984; Fortin & Brezzi, 1986). Both dual formulation of Stokes equations and primal formulation of Darcy equations are discretised by using the MINI-element or P1+/P1-element which has demonstrated its stability (Celle et al., 2008b). This mixed element consists in a linear approximation of both velocity and pressure with a bubble enrichment of the velocity field on each element. The bubble function vanishes on the element edges, and its associated degree of freedom is removed by static condensation. Thus, the MINI-element results finally in a linear approximation of both velocity and pressure (P1/P1 approximation) with a stabilisation term induced by the bubble condensation. Unlike penalisation methodology, the stabilisation term depends here on both physics and discretisation of the problem to be solved.

4.3 *Coupling conditions*

For the Stokes–Darcy coupling, the regions where Stokes and Darcy flows prevail are considered independent and an iterative process ensures the equilibrium between these two regions where the flows have been solved (Discacciati & Quarteroni, 2009). In the iterative process, a special attention has to be paid regarding the Stokes–Darcy velocity jump across the interface, of several decades in severe regimes, which can lead to solving of the ill-conditioned systems. Let us have a look to the coupling conditions by themselves.

4.3.1. *Continuity of normal velocity for low permeability media*

When normal or tangential conditions are prescribed for pressure or velocity (Figure 2), the penalty method is classically used to enforce the corresponding relationships between the dofs involved, with the help of a penalty factor. Specifically, the relationship is added to the degree of freedom associated with the largest normal vector

coordinates (n_x or n_y or n_z) in order to keep dominant diagonal system. But in general cases, where normals are not different enough, *i.e.* for local normals not aligned at all on global coordinate axes, extra diagonal terms can appear after the system conditioning. However, this can be easily avoided if this condition is written in a local system of coordinates different from the global frame, requiring some light local rotations for the dofs concerned, pre-processing from global to local frame and post-processing from local to global frames. Then, a linear constraint over the degrees of freedom associated with this condition will appear in the system diagonal only, preserving the diagonal dominant nature.

Consider an interface with a local normal $\mathbf{y}$. Prescribing the normal velocity continuity will lead to a condition to be enforced, when solving $\mathbf{AX} = \mathbf{B}$, which will look like:

$$\cdots + (a_{l,k} + \lambda n_y) v_{y,s} + \cdots = b_l + v_{y,d}\ n_y\ \lambda \tag{36}$$

where λ is the coefficient of penalisation, and $a_{l,k}$, b_l are the coefficients of the global matrices. However, when using this formulation (36), the continuity of the normal velocity is lost for small values of permeability.

This comes from the fact that in this relationship the penalty coefficient, classically taken as 10^{8-12} max $(a_{l,k})$, is multiplied by the permeability, which is in the range $[10^{-8}, 10^{-14}]\mathrm{m}^2$ in the applications concerned with this paper. The constraint is then too weak to ensure velocity continuity, and consequently mass conservation. To overcome this difficulty, the penalty coefficient can be solely chosen with respect to the permeability as $\lambda = \frac{10^5}{K}$. Various tests for different values of permeability, viscosity and thickness of fluid layer were conducted and results are shown in subsection 6.1 for instance.

4.3.2. *Condition on tangential velocity*

Beavers and Joseph (1967) proposed a condition postulating that the difference between the slip velocity of the free fluid and the tangential component of the seepage velocity is proportional to the shear rate of the free fluid, as stated in Equation (5). For pragmatic reasons, in the presented form, the Beavers joseph Saffman condition disregards the Darcy's velocity contribution. Consequently, for the decoupled approach that is under consideration, no corresponding external constraint will appear in the Stokes weak formulation and hence the effect of the Darcy regime onto the Stokes flow cannot be accounted for.

Then, a BJS-like condition is introduced. In our iterative scheme, the Darcy contribution can be easily introduced, by considering the Darcy's velocity computed at the previous iteration $i-1$:

$$2\mathbf{n} \cdot \dot{\boldsymbol{\varepsilon}}(\mathbf{v_s})^i \cdot \boldsymbol{\tau}_\mathbf{j} = \frac{\alpha}{\sqrt{K}} (\mathbf{v}_\mathbf{s}^i - \mathbf{v}_\mathbf{d}^{i-1}) \cdot \boldsymbol{\tau}_\mathbf{j} \tag{37}$$

with $\boldsymbol{\tau}_\mathbf{j}$ vectors tangent to the interface. Let us notice that for normal flow-dominated problems, this velocity will naturally vanish.

4.4. *Iterative coupling*

As stated previously, an iterative scheme is used to equilibrate both flows in Stokes and Darcy regions through interface conditions. The dual Stokes and primal Darcy formulations have been selected for their stability property but also for accessing properly the Dirichlet boundary conditions in order to fulfil these interface conditions.

The iterative process can be described such as in Algorithm 1. First, the Stokes problem is solved for v_s^i under the condition of normal velocity continuity and BJS-like tangential velocity (Equation (37)) on interface Γ_s, knowing the Darcy velocity at the previous iteration $\mathbf{v_d}^{i-1}$ on Γ_d. Second, the Darcy problem is solved for $\mathbf{v_d}^i$ under the condition of pressure continuity on interface Γ_d, knowing on Γ_s the Stokes pressure p_s^i previously determined. The iterative process terminates when both velocity and pressure corrections get smaller than a given residual ϵ

$$\frac{1}{N_i}\sum_{j=1}^{N_i}\left(\left|\frac{v_j^{i+1}-v_j^i}{v_j^{i+1}}\right|+\left|\frac{p_j^{i+1}-p_j^i}{p_j^{i+1}}\right|\right)<\epsilon \tag{38}$$

where N_i is the total number of nodes at the interface, i is the iteration index, v_j^i and p_j^i are, respectively, the normal velocity and pressure at node j of the interface.

Algorithm 1 Iterative scheme for the decoupled approach

$i \leftarrow 0$
Enforce an initial condition $\mathbf{v_d}^i = 0$ on interface Γ_d.
$i \leftarrow 1$
While not convergence **do**
  Find $(\mathbf{v_s}^i, p_s^i)$ solutions of Stokes dual formulation with Dirichlet boundary conditions imposed by permeability-controlled penalty:

- $\mathbf{v_s}^i \cdot n = \mathbf{v_d}^{i-1} \cdot n$ on Γ_s
- $(2\mathbf{n}\cdot\dot{\boldsymbol{\varepsilon}}(\mathbf{v_s}^i) - \frac{\alpha}{\sqrt{K}}\mathbf{v_s}^i)\cdot\boldsymbol{\tau}_\mathbf{j} = -\frac{\alpha}{\sqrt{K}}\mathbf{v_d}^{i-1}\cdot\boldsymbol{\tau}_\mathbf{j}, \quad j=1,2$ on interface Γ_s.

  Find $(\mathbf{v_d}^i, p_d^i)$ solutions of Darcy equation with Dirichlet boundary condition:
  $p_d^i = p_s^i$ on Γ_d
  if convergence (Equation (38)) **then**
    Exit
  else
    $i \leftarrow i+1$
  end if
end while

5. Method of manufactured solutions

To verify implementation and convergence of both approaches, the method of manufactured solution (Salari & Knupp, 2002) was used. It consists in building an analytical solution that is fed into the system of equations under consideration and permits to calculate the corresponding right-hand-side term. This term is subsequently implemented into the numerical code to obtain the numerical solution of the discrete problem. Finally the difference between the general analytical solution and the numerical one is calculated and permits to assess the capability of the method to solve the PDE set of equations. To verify Stokes–Darcy coupling, a Stokes–Darcy coupled problem is studied. Regular meshes are used to obtain the numerical solution. The studied area is divided into $1/h$ squares, where h is the mesh size. Each square is itself divided into two triangles. Several meshes are used: 10×10, 20×20, 40×40 and 80×80. Each grid corresponds to a more refined version of the previous one.

Remark: In all the numerical tests, the numerical constants considered for the monolithic approach are taken as: $c_1 = 1$, $c_u = c_p = 2$ and $L_0 = \sqrt[m]{meas(\Omega_d)}$.

5.1. *Stokes–Darcy coupled problem*

Stokes–Darcy coupled problem is conducted in the domain $\Omega = [0, 1] \times [0, 1]$ with $\Omega_s = [0, 0.5] \times [0, 1]$ and $\Omega_d = [0.5, 1] \times [0, 1]$; let's consider the following velocity and pressure fields

$$\begin{aligned} v_{x,s} &= y^4 e^x \\ v_{y,s} &= -1/5 y^5 e^x \\ p_s &= -y^4 e^x \\ v_{x,d} &= y^4 e^x \\ v_{y,d} &= -1/5 y^3 e^x \\ p_d &= -y^4 e^x \end{aligned} \tag{39}$$

Zero-velocity Dirichlet conditions are prescribed on the overall boundary of the domain Ω. For each mesh, and each numerical solution v_h and p_h, the errors are calculated using the following norms.

- Norm L^2:

$$\|u\|_{0,\Omega} = \left(\int_\Omega u^2 d\Omega \right)^{1/2} \tag{40}$$

- Norm H^1:

$$\|u\|_{1,\Omega} = \left(\|u\|_{0,\Omega}^2 + \sum_{j=1}^{m} \left\| \frac{\partial u}{\partial x_j} \right\|_{0,\Omega}^2 \right)^{1/2} \tag{41}$$

The errors allow calculating the rate of the convergence. For Stokes equations, using linear approximation for elements, the rate of the convergence satisfies (Girault & Raviart, 1979).

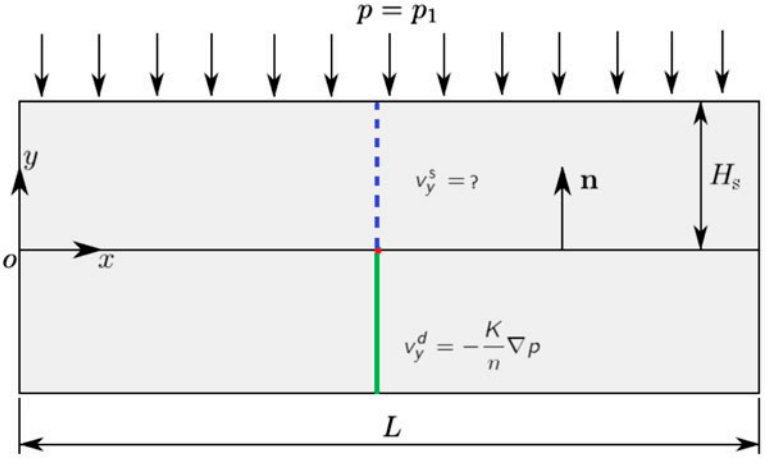

Figure 2. Normal velocities in Stokes and Darcy media.

$$\|\mathbf{v} - \mathbf{v_h}\|_{1,\Omega_s} + \|p - p_h\|_{0,\Omega_s} \leq C\ h(\|\mathbf{v}\|_{2,\Omega_s} + \|p\|_{1,\Omega_s}) \tag{42}$$

where C is the constant and $\|\cdot\|_{2,\Omega}$ is the H^2 norm defined as:

$$\|u\|_{2,\Omega} = \left(\|u\|^2_{0,\Omega} + \sum_{j=1}^{m} \left\| \frac{\partial u}{\partial x_j} \right\|^2_{0,\Omega} + \sum_{i,j=1}^{m} \left\| \frac{\partial^2 u}{\partial x_i x_j} \right\|^2_{0,\Omega} \right)^{1/2} \tag{43}$$

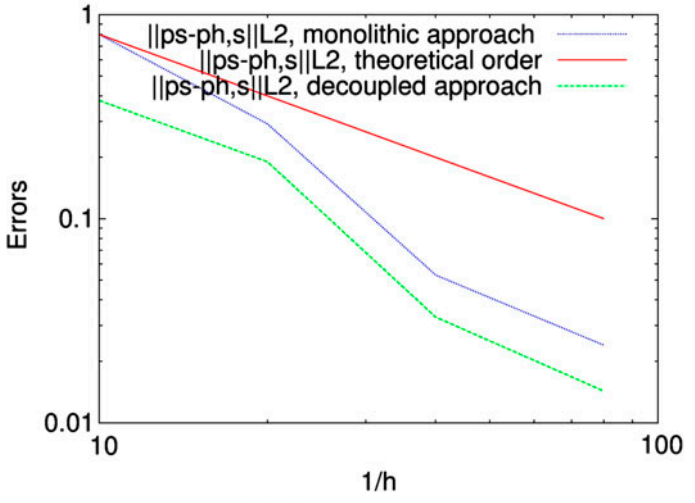

(a) Pressure

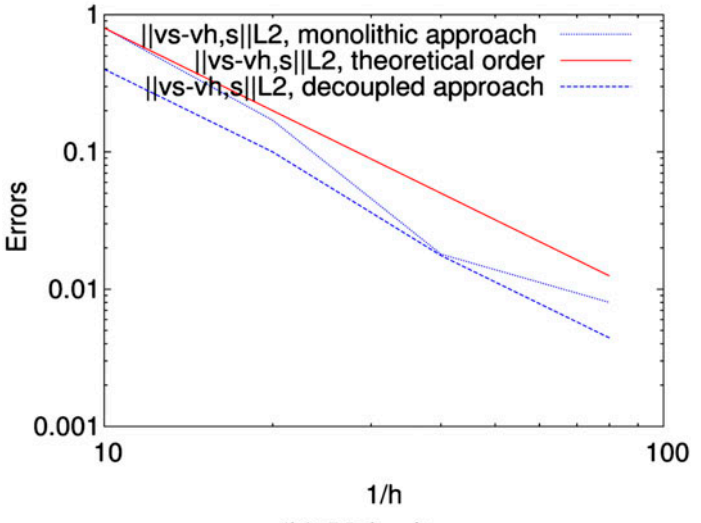

(b) Velocity

Figure 3. (a) Convergence of the error for the pressure (theoretical order of convergence = 1 (Girault & Raviart, 1979)) and (b) velocity in Stokes domain for coupled problem (theoretical order of convergence = 2 (Girault & Raviart, 1979)) with h the size of mesh $\eta = 1$ Pa s, $K = 1$ m^2, $\alpha = 1$.

For the dual formulation of Darcy problem, using linear approximations for both velocity and pressure, the rate of the convergence has to satisfy (Karper, Mardal, & Winter, 1991)

$$\|\mathbf{v} - \mathbf{v_h}\|_{H(div,\Omega_d)} + \|p - p_h\|_{0,\Omega_d} \leq C\ h(\|\mathbf{v}\|_{2,\Omega_d} + \|p\|_{1,\Omega_d}) \tag{44}$$

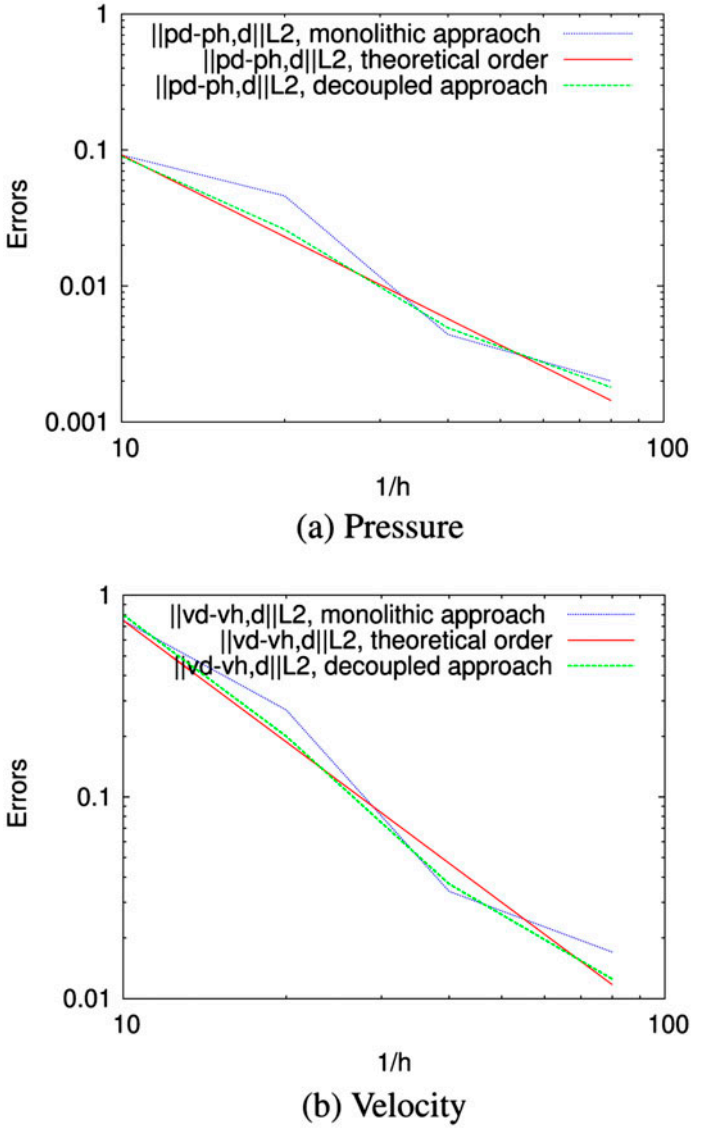

Figure 4. Convergence of the error for the pressure (a) (theoretical order of convergence = 2 (Girault & Raviart, 1979)) and velocity (b) (theoretical order of convergence = 2 (Girault & Raviart, 1979)) in Darcy domain for coupled problem with h the size of mesh $\eta = 1$ Pa s, $K = 1$ m^2, $\alpha = 1$.

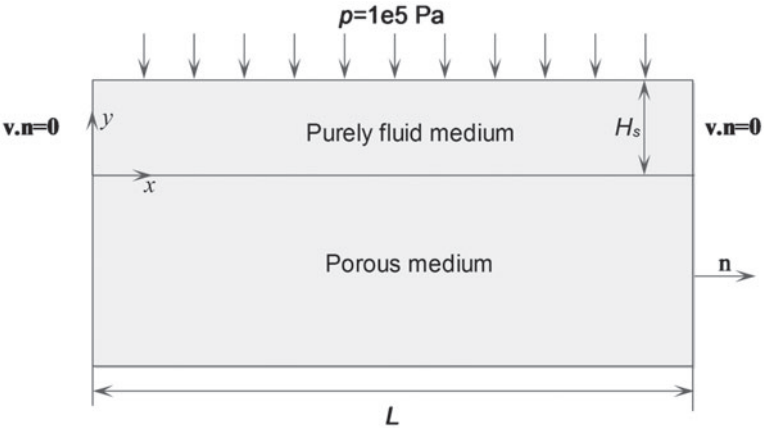

Figure 5. Boundary conditions for a flow perpendicular to the interface, $\alpha = 1$, $\eta = 1$ Pa s.

And for the primal formulation of Darcy problem, using linear approximations, the rate of the convergence has to satisfy

$$\|\mathbf{v} - \mathbf{v_h}\|_{0,\Omega_d} + \|p - p_h\|_{H^1,\Omega_d} \leq C\ h(\|\mathbf{v}\|_{1,\Omega_d} + \|p\|_{2,\Omega_d}) \tag{45}$$

where C is a constant.

An analysis of the convergence is carried out for both pressure and velocity in the subdomains Ω_s and Ω_d. The convergence of the error for both pressure and velocity in Stokes domain is represented in log scale in Figure 3. For pressure in Stokes region (Figure 3(a)), the rate of convergence in norm L^2 for monolithic approach is

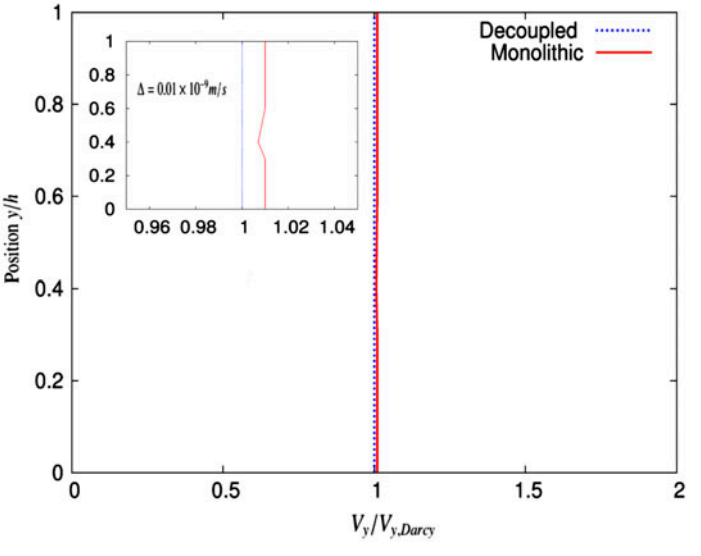

Figure 6. Normalised normal velocity v_y for viscosity $\eta = 1$ Pa s with a permeability of $K = 10^{-14}\text{m}^2$ and $\alpha = 1$.

Table 1. Relative errors for normal velocities in Stokes region for monolithic and decoupled approaches, K = 10^{-14} m^2, perpendicular flow corresponding to Figure 5.

h (m)	$\|v_{y,error}\|_{monolithic}$ (%)	$\|v_{y,error}\|_{decoupled}$ (%)
100 × 25	0.468	0.401
100 × 50	0.231	0.211
100 × 100	0.141	0.109
100 × 200	0.111	0.099

[1.13:2.45] (theoretical order is 1) while the rate of convergence for decoupled approach is [1.2:2.5].

For Stokes velocity (Figure 3(b)), the rate of convergence is [1.14:3.2] in norm L^2 for monolithic approach. A superconvergence is noticed when mesh size goes from $h = 0.05$ to $h = 0.025$ due again to the optimal choice of the constant c_1. The rate of convergence decreases when mesh size $h = 0.025$ becomes $h = 0.0125$, while for the decoupled approach the rate of convergence for velocity is [2:2.5]. Also, an analysis of the convergence is carried out for both pressure and velocity in the Darcy subdomain Ω_d Figure 4. The convergence rates for pressure are [1.14:3.3], for the monolithic approach and [1.4:2.4] for the decoupled approach (theoretical rate is of order 2), and for the velocity it is [1.1:2.98] for the monolithic approach and [1.6:2.4] for the decoupled approach (theoretically it is of order 2). For the monolithic approach, the rate of convergence is relatively high due to the 'optimal' choice of constants c_p, c_u and c_1 in the stabilisation terms $\tau_{u,c}$ and $\tau_{p,c}$ (Badia & Codina, 2008). The superconvergence of both methods is noticed when we pass from $h = 0.05$ drops to $h = 0.025$, but it is more important in the monolithic approach due to the optimal choice of the constants c_u, c_p

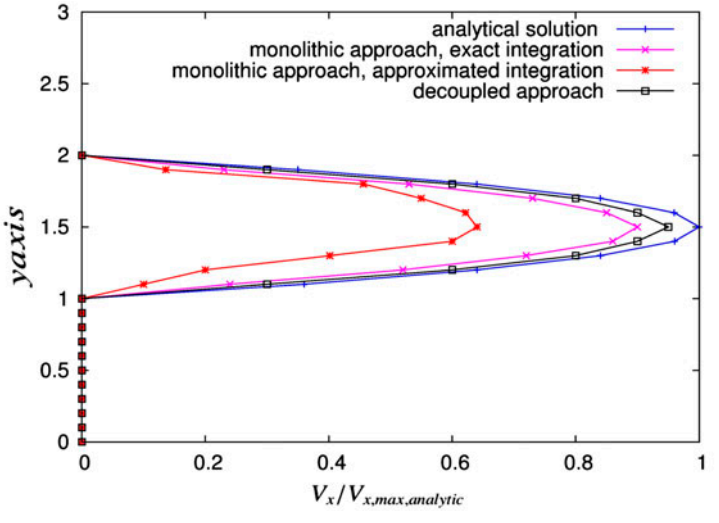

Figure 7. Comparison of numerical solutions for both monolithic and decoupled approaches for a parallel flow, with analytical solution. Velocity is normalised by the maximum analytical velocity ($\mathbf{v}_{x,max,analytic}$). For the monolithic approach, interface reconstruction and Dirac approximation for the surface integral are presented. For the decoupled approach, the interface is explicitly known through the interface mesh ($K = 10^{-14}\text{m}^2, p_{ext} = 1bar, \eta = 1$ Pa s, $\alpha = 1$).

and L_0 in the stabilisation terms $\tau_{u,c}$ and $\tau_{p,c}$. These results correspond to the theoretical and numerical convergence rates determined in Karper et al. (1991).

6. Numerical tests and comparisons

These simulations have been carried out by using the finite element software Z-set[1] (Besson & Foerch, 1997) for the monolithic approach and the industrial code PAM-RTM from ESI Group for the decoupled approach. Different tests are conducted here to highlight the characteristics and advantages of each method.

6.1. *Perpendicular flow*

A series of studies was conducted for the case of the fluid flow perpendicular to the interface corresponding to Figure 5 with known analytical solution, where

$$\begin{aligned} v_{x,s} &= v_{x,d} = 0, \\ v_{y,s} &= v_{y,d} = -\tfrac{K}{\eta}\nabla p_d, \\ p_s &= 10^5\ Pa \\ p_d &= 10^5\, y\ Pa \end{aligned} \tag{46}$$

Let us consider a domain $\Omega = [0;5] \times [0;2]\ m^2$ made up of two sub-domains: a pure fluid domain $\Omega_s = [0;5] \times [1;2]\ \mathrm{m}^2$ and porous medium $\Omega_d = [0;5] \times [0;1]\ \mathrm{m}^2$. Boundary conditions are presented in Figure 5. For comparison purpose, Δ is defined as the largest difference between velocities computed with decoupled and monolithic approaches.

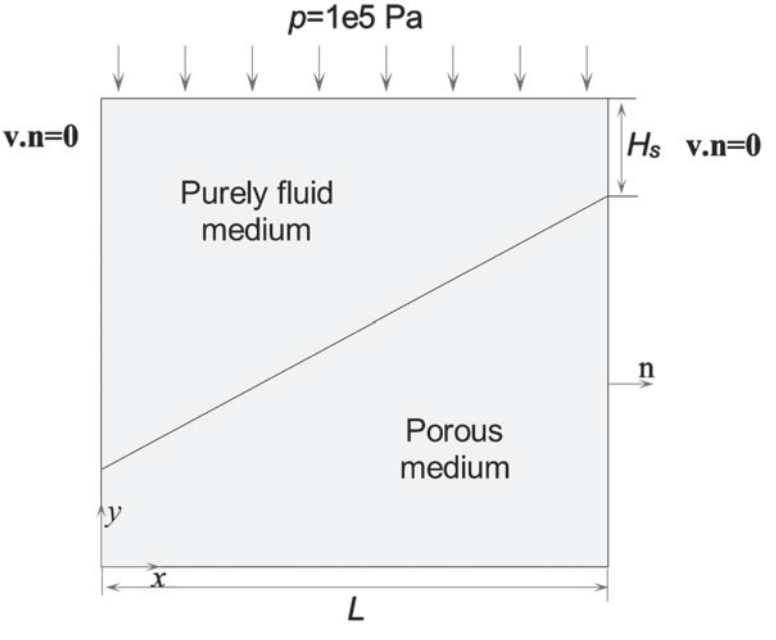

Figure 8. Geometry and boundary conditions for the case with inclined interface, $\eta = 1$ Pa s, $K = 10^{-15}\mathrm{m}^2$ and $\alpha = 1$.

Figure 6 presents the normal velocities obtained with both monolithic and decoupled approaches in the domain Ω, normalised by normal velocity in the Darcy medium, $\eta = 1$ Pa s, $\alpha = 1$. As it can be seen, in both approaches the continuity of the normal velocity is verified. The slight difference Δ between values of normal velocity computed with both decoupled and monolithic approaches is in the range $[4\ 10^{-12};\ 1.3\ 10^{-12}]\mathrm{m\,s^{-1}}$ for a permeability $K = 10^{-14}\ \mathrm{m}^2$.

Convergence of the solution, as well as relative errors, have been considered for the test case of the perpendicular flow. The obtained numerical results were compared with analytical ones. The errors were computed: $\|u_{error}\| = \frac{\|u_a - u_h\|_0}{\|u_a\|_0}$, where u_a is the analytical solution and u_h is the obtained numerical solution. Results in terms of Stokes velocity for different sizes of mesh were obtained, when $\eta = 1$ Pa s, $K = 10^{-14}\ \mathrm{m}^2$ and are presented in Table 1. It can be verified that both methods are robust and lead to very similar relative error which becomes smaller when the mesh becomes finer.

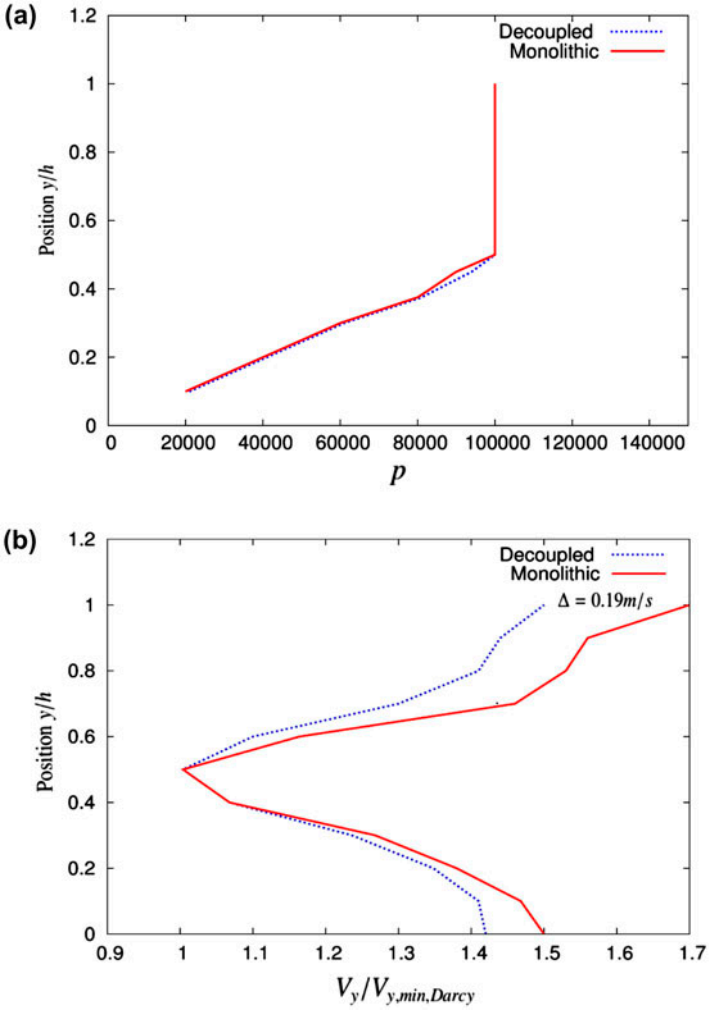

Figure 9. (a) Pressure p and (b) normalised normal velocity v_y for $\eta = 1\ Pa.s$, $K = 10^{-15}\ \mathrm{m}^2$ and $\alpha = 1$. Results corresponding to the inclined interface case (Figure 8).

6.2. *Parallel flow*

The case of parallel flow is used to validate the capability of both approaches to satisfy the interface condition on tangential velocity (BJS). To deal with a flow parallel to the interface, let us consider the same geometry as in Figure 5 with different boundary conditions: a domain Ω made up of two sub-domains, a purely fluid domain $\Omega_s = [0;5] \times [1;2]$ m and porous medium $\Omega_d = [0;5] \times [0;1]$ m^2. A pressure gradient p of $10^5\,Pa$ is applied along the x-axis. Other boundary conditions are zero velocity on top and bottom sides of the geometry.

Results for the permeability of the porous medium $K = 10^{-14}\,\mathrm{m}^2$, viscosity $\eta = 1$ Pa s, slip coefficient $\alpha = 1$ are presented in Figure 7.

It can be verified that velocities computed with decoupled approach coincide with the analytical profile. Results obtained with the monolithic approach are also in good correlation with analytical ones provided the surface integral is computed exactly. Moreover, the difference in the tangential velocity follows from the mixture of elements on the interface belonging to both Stokes and Darcy domains in the monolithic approach. Results for other values of permeability do not differ much in the aspect of flow in Stokes region due to the nature of the 'Poiseuille' flow for the low permeabilities considered.

6.3. *Inclined interface*

To study further the capabilities of the coupling conditions for interfaces which are not parallel to some groups of mesh element faces, hence implying linear relationships between the velocity dofs (Equation (37)), the case of an inclined interface is considered. A domain $\Omega = [0;1] \times [0;1]$ m^2 is made up of two sub-domains: a purely fluid domain Ω_s, where $H_s = [0.2;\ 0.8]$ m and porous medium Ω_d. Geometry as well as the boundary conditions on $\partial\,\Omega$ in velocity and pressure are shown in Figure 8.

A range of numerical tests were conducted, where permeability of the porous medium was varied down to $10^{-15}\,\mathrm{m}^2$, $\eta = 1$ Pa s and $\alpha = 1$. Results for the pressure and velocity field obtained by both approaches are presented in Figure 9. A good correlation can be noticed for both studied methods ($\Delta = 1.89\ 10^{-7}\mathrm{m/s}$).

7. Complex geometries

The Stokes–Darcy coupled problem is used here to simulate stationary stages in complex composite pieces elaborated through infusion processes (Celle et al., 2008a,

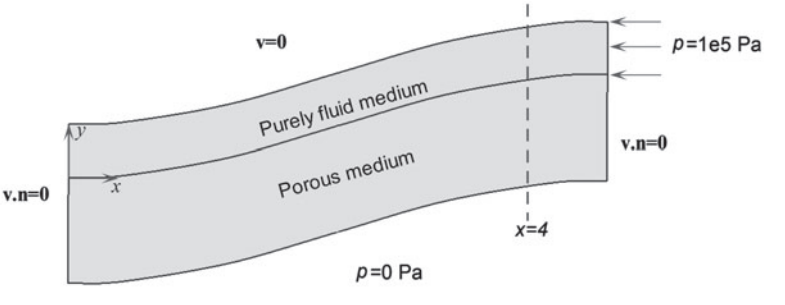

Figure 10. Geometry and boundary conditions for the 2D piece with curved interface, $K = 10^{-11}\mathrm{m}^2$, $\alpha = 1$ and $\eta = 1\ Pa.s$.

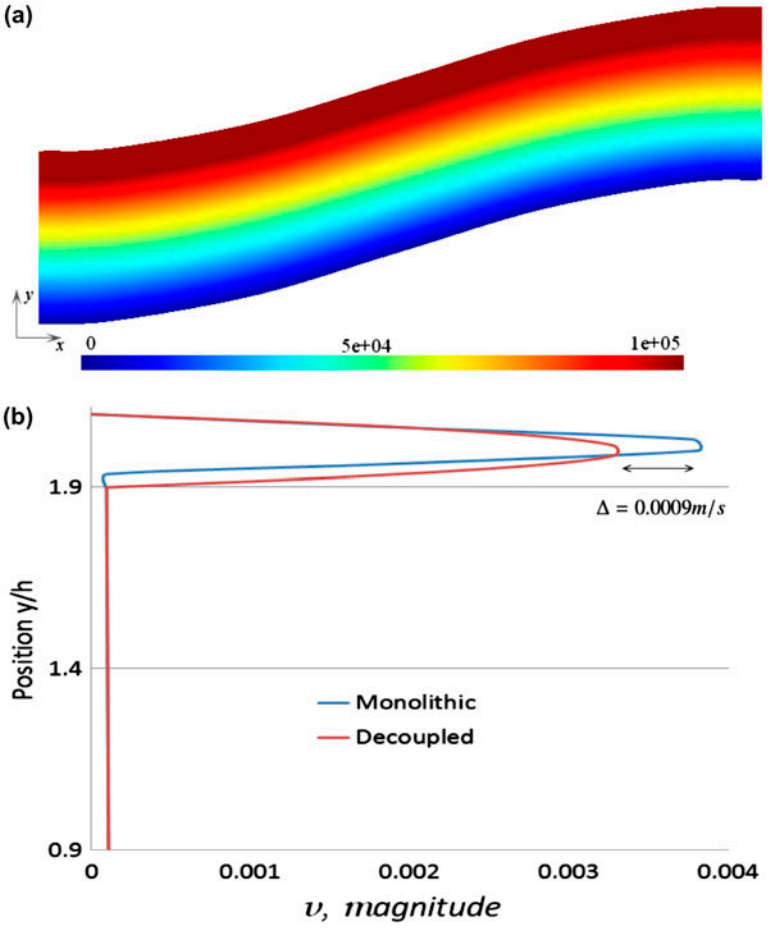

Figure 11. (a) Pressure field and (b) velocity magnitude when $x = 4$ for permeability $K = 10^{-11}$ m^2, $\eta = 1$ *Pa.s*, $\alpha = 1$, 2D complex piece.

2008b; Wang, Molimard, Drapier, Vautrin, & Minni, 2012). Previously, the mathematical models for this simulation were derived and two approaches were validated using the tests, where analytical solution is available, i.e. tests with simple geometry. But in infusion processes, pieces with complex geometries are to be considered. In this section, coupled problems for 2D and 3D pieces with complex geometries are investigated.

7.1. 2D simulation

A case deriving from the parallel flow is first used, exhibiting a 2D curved interface (Figure 10) with $K = 10^{-11}$ m^2, $\eta = 1$ *Pa.s* and $\alpha = 1$ and for a Stokes region thickness of $\frac{1}{10}$ of the total thickness. Results for pressure field presented coincide for monolithic and decoupled approach in Figure 11(a). Magnitude of velocity is plotted over the line $x = 4$ for both monolithic and decoupled approaches in Figure 11(b). A good correlation between results can be noticed, and the slight difference close to the interface comes

from the different ways of enforcing interface conditions, the same as for the case of parallel flow (here $\Delta = 0.005$ m/s).

7.2. 3D simulation

For the 3D flow in a piece with complex geometry, a simulation was conducted for $K = 10^{-9}$ m^2, $\eta = 1$ *Pa.s* and $\alpha = 1$. Geometry and mesh and boundary conditions are presented in Figure 12(a) and (b) for the decoupled and monolithic approaches,

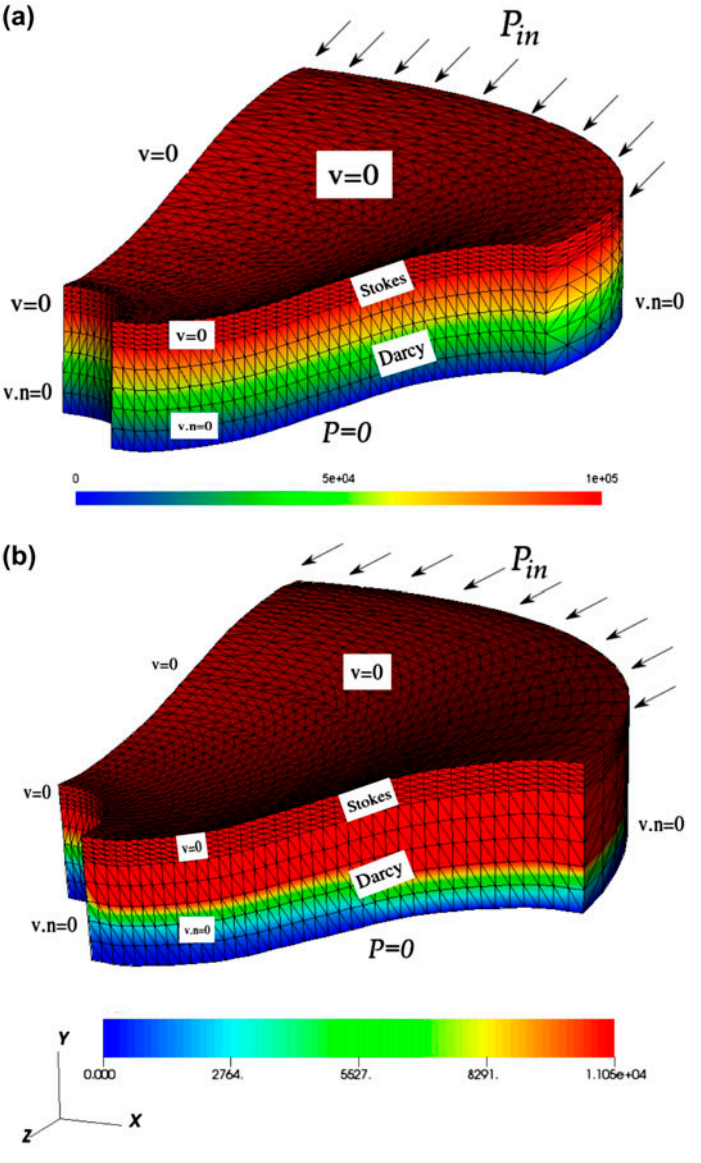

Figure 12. (a) Pressure field for the decoupled approach and (b) for the monolithic approach for permeability $K = 10^{-9}$ m^2, $\eta = 1$ *Pa.s*, $\alpha = 1$, 3D complex piece.

respectively. Geometry consists in two layers – layer of thickness 2 mm that corresponds to the Stokes region, and layer of thickness 10 mm that corresponds to Darcy region. For the boundary conditions, pressure is prescribed on the right-hand-side in Stokes region, and vent is present on the bottom of Darcy region. Also conditions of zero velocity for Stokes region and zero normal velocities for Darcy region are prescribed for all the other boundaries of the piece. The stationary case, presented in Figure 12, illustrates the capability of representing realistic geometries with both decoupled and monolithic approaches. Presented results for pressure fields, for both approaches, as well as results for velocity fields are in accordance with expected results.

7.3. Required computation time of the results

Difference in meshing scheme and weak formulation in both studied approaches causes also some difference in computational algorithm, and therefore difference in CPU time. As it was described previously, the decoupled approach is based on an iterative process. Stokes and Darcy systems are constructed separately and, at least two iterations are required to reach the global convergence. However, the sizes of the Stokes and Darcy systems are smaller than the one of the monolithic approach system. Consequently, it could be interesting to compare the time cost of each method. Nevertheless, it is really difficult to compare two methods implemented in two different finite element codes. Many parameters, not necessarily related to the numerical method, can be involved in the CPU time cost. This difficulty is increased when the two methods are applied on different meshes, as in our case. For the simulations presented in this paper, the CPU time ratio between the decoupled approach (with a precision $\varepsilon = 10^{-5}$) and the monolithic approach is around two or three. Moreover, in realistic infusion process simulations which is the context of this work, the Stokes domain is very small compared to the Darcy domain. Consequently, if Stokes CPU time can be neglected, we can suppose that solving twice the Darcy equations will always take more time than solving one time the Stokes–Darcy coupled problem (which in this case has almost the cost of the Darcy problem alone).

8. Conclusion

A monolithic and a decoupled strategy have been presented to solve the Stokes–Darcy coupled problem. In the monolithic approach, a single unstructured mesh is used to compute the Stokes and Darcy (in the dual form) contributions to the global algebraic system. Both velocity and pressure are approximated by linear finite elements. The LBB stability conditions are circumvented by using the VMS method and the ASGS method. In the decoupled approach, two meshes matching at the interface are considered. Using a convergence loop, Stokes and Darcy (primal form) problems are alternatively solved, using the MINI-element until reaching the global equilibrium.

Tests with different types of boundary conditions and geometry were conducted, to verify the coupling conditions, i.e. continuity of normal velocity and BJS condition on tangential velocity. It was shown that the implemented approaches provide a good agreement with analytical solution for the test cases of perpendicular and parallel flows with permeability down to $10^{-15}\,\mathrm{m}^2$, different values of fluid viscosity and thin thickness of fluid layer. Convergence rates have been investigated with manufactured solution method, showing the accuracy of both methods and recovering the theoretical

results. The novelty of these approaches lies in their ability to deal with very low permeabilities, complex geometries closed to industrial applications. Both coupled and decoupled approaches have shown their ability to describe accurately the flow of a Newtonian fluid in a Stokes–Darcy medium.

This work can be improved by considering an anisotropic porous medium and consequently a second-order permeability tensor. Decoupled and monolithic approaches have to be extended to treat this configuration. Especially, the stabilisation parameters must be adapted. Finally, the evolution of the flow front can take into account through an interface capturing method. This work has been performed in reference (Abouorm, Moulin, Bruchon, & Drapier, 2013) using the level-set method. In this case, the monolithic approach seems to be more efficient than the decoupled one.

Note

1. This C++ code is developed mainly by Ecole des Mines de Paris, Office National d'Etudes et de Recherches Aérospatiales (ONERA), Ecole des Mines de Saint-Etienne and the Northwest Numerics and Modelling company.

References

Abouorm, L., Moulin, N., Bruchon, J., & Drapier, S. (2013). Monolithic approach of Stokes–Darcy coupling for LCM process modelling. *Key Engineering Materials, 554–557*, 447–455.

Arnold, D., Brezzi, F., & Fortin, M. (1984). A stable finite element for the Stokes equations. *Calcolo, 21*, 337–344.

Badia, S., & Codina, R. (2008). Unified stabilized finite element formulation for the Stokes and the Darcy problems. *SIAM Journal on Numerical Analysis, 47*, 1971–2000.

Badia, S., & Codina, R. (2010). Stabilized continuous and discontinuous Galerkin techniques for Darcy flow. *Computer Methods in Applied Mechanics and Engineering, 199*, 654–1667.

Beavers, G., & Joseph, D. (1967). Boundary conditions at a naturally permeable wall. *Journal of Fluid Mechanics, 30*, 197–207.

Besson, J., & Foerch, R. (1997). Large scale object-oriented finite element code design. *Computer Methods in Applied Mechanics and Engineering, 142*, 691–706.

Bruchon, J., Digonnet, H., & Coupez, T. (2009). Using a signed distance function for the simulation of metal forming processes: Formulation of the contact condition and mesh adaptation. from a lagrangian approach to an eulerian approach. *International Journal for Numerical Methods in Engineering, 78*, 980–1008.

Burman, E., & Hansbo, P. (2007). A unified stabilized method for Stokes' and Darcy's equations. *Journal of Computational and Applied Mathematics, 198*, 35–51.

Celle, P., Drapier, S., & Bergheau, J. (2008a). Numerical aspects of fluid infusion inside a compressible porous medium undergoing large strains. *European Journal of Computational Mechanics, 17*, 819–827.

Celle, P., Drapier, S., & Bergheau, J. (2008b). Numerical modelling of liquid infusion into fibrous media undergoing compaction. *European Journal of Mechanics – A/Solids, 27*, 647–661.

Discacciati, M., & Quarteroni, A. (2009). Navier-Stokes/Darcy coupling: Modeling, analysis, and numerical approximation. *Revista Metematica Complutense, 22*, 315–426.

Fortin, M., & Brezzi, F. (1986). *Mixed and hybrid finite element method*. Berlin: Springer.

Girault, V., & Raviart, P.-A. (1979). *Finite element approximation of the Navier-Stokes equations*. Lecture notes in mathematics. Springer.

Hughes, T. (1995). Multiscale phenomena: Green's functions, the Dirichlet-to-Neumann formulation, subgrid scale models, bubbles and the origins of stabilized methods. *Computer Methods in Applied Mechanics and Engineering, 127*, 387–401.

Hughes, T., Feijóo, G., Mazzei, L., & Quincy, J. (1998). The variational multiscale method – A paradigm for computational mechanics. *Computer Methods in Applied Mechanics and Engineering, 166*, 3–24.

Karper, T., Mardal, K.-A., & Winter, R. (1991). Unified finite element discretizations of coupled Darcy-Stokes flow. *Numerical Methods for Partial Differential Equations, 25*, 311–326.

Layton, W. J., Schieweck, F., & Yotov, I. (2003). Coupling fluid flow with porous media flow. *SIAM Journal on Numerical Analysis, 40*, 2195–2218.

Osher, S. (1988). Fronts propagating with curvature-dependent speed: Algorithms based on Hamilton-Jacobi formulations. *Journal of Computational Physics, 79*, 12–49.

Pacquaut, G., Bruchon, J., Moulin, N., & Drapier, S. (2012). Combining a level-set method and a mixed stabilized P1/P1 formulation for coupling Stokes–Darcy flows. *International Journal for Numerical Methods in Fluids, 69*, 459–480.

Pino Muñoz, D., Bruchon, J., Drapier, S., & Valdivieso, F. (2013). A finite element-based level set method for fluid-elastic solid interaction with surface tension. *International Journal for Numerical Methods in Engineering, 93*, 919–941.

Salari, K., & Knupp, P. (2002). *Computational methods in transport: Verification and validation, Computational science and engineering*.

Sussman, M., Smereka, P., & Osher, S. (1994). A level set approach for computing solutions to incompressible two-phase flow. *Journal of Computational Physics, 114*, 146–159.

Wang, P., Molimard, J., Drapier, S., Vautrin, A., & Minni, J. (2012). Monitoring the resin infusion manufacturing process under industrial environment using distributed sensors. *Journal of Composite Materials, 46*, 691–706.